JOURNAL OF Applied Polymer SCIENCE

Acrylic Hydrogels-Based Biocomposites: Synthesis and Characterization

Teodor Sandu,[1,2] Andrei Sârbu,[2] Floriana Constantin,[1] Silviu Vulpe,[3] Horia Iovu[1]

[1]Department of Bioresources and Polymer Science, University "Politehnica," Calea Victoriei 149, Bucharest 010072, Romania

[2]National Research-Development Institute for Chemistry and Petrochemistry—ICECHIM, Splaiul Independentei 202, sector 6, PO Box 174/35, Bucharest 060021, Romania

[3]Physics Faculty, University of Bucharest, Atomiştilor 405, Măgurele, Ilfov 077125, Romania

Correspondence to: A. Sârbu (E-mail: andr.sarbu@gmail.com)

ABSTRACT: Hydrogels based on polyacrylic and polymethacrylic acids were synthesized using two variants of redox initiating systems and three crosslinking agents in various ratios to the monomer. The chemical structure of these hydrogels was extensively studied by Fourier transform infrared (FTIR) spectrometry and Raman spectrometry. These hydrogels were also characterized by other techniques, namely thermo gravimetric analysis (TGA), differential thermal gravimetry, differential scanning calorimetry (DSC), and scanning electron microscopy (SEM). The hydrogel ability to immobilize enzymes through covalent bonds was studied by FTIR and Raman spectrometry and by analyzing the SEM images before and after enzyme immobilization. The enzyme influence on the thermal behavior of the hydrogel biocomposite was investigated by DSC and TGA, too. The methacrylic acid leads to more thermo stable hydrogels formation than acrylic acid. Acrylic and methacrylic hydrogels are able to covalently immobilize enzymes. This is proved by the important changes which occur in the chemical composition, the thermal behavior and the morphology of hydrogels after immobilization stage. © 2012 Wiley Periodicals, Inc. J. Appl. Polym. Sci. 000: 000–000, 2012

KEYWORDS: biomaterials; gels; hydrophilic polymers; proteins

Received 23 February 2012; accepted 2 May 2012; published online
DOI: 10.1002/app.37992

INTRODUCTION

Hydrogels are crosslinked polymer three-dimensional networks produced by the simple reaction of one or more monomers and/or by using the synthetic, semisynthetic or natural polymers, separately or in combination, being able to absorb large quantities of water, saline solutions or physiological fluids, without dissolving or losing their structural integrity, being yet insoluble, due to the physical and chemical crosslinkings, entanglements, or crystalline regions.[1–9] Hydrogels can be synthesized by radiation (γ or UV) initiating, grafting polymerization or freeze-thawing, using copolymers, poly(ethylene glycol) (PEG), poly(dimethyl siloxane) (PDMS), carboxymethyl cellulose (CMC), 2-hydroxyethyl methacrylate (HEMA), *N*-vinyl polypyrrolidone (NVP), acrylic acid (AA). Poly (acrylic acid) (PAA) hydrogels, a basis of the superabsorbent material class, are used for coatings and interpenetrating polymer networks (IPNs).[2,6–8,10–23]

Enzymes are widely used as catalysts, for biosensors and bioremediation due to their good specificity, but their usage is limited because of the short catalytic lifetimes. Enzyme immobilization represents a way to overcome this drawback, facilitating its separation from reaction mixture and its reuse in new reaction cycles, being, also possible to use enzymes in multienzyme and chemoenzymatic cascade processes and to reduce significantly the operation costs.[24–29] The immobilization on different supports (organic polymers, biopolymers, hydrogels, inorganic supports, smart polymers) can be performed by chemical (covalent bonds) and physical methods (adsorption, entrapment, microencapsulation).[19,24] The advantage of hydrogels consists of the soft and fluid environment of fully hydrated hydrogel assuring near-physiological conditions for the enzyme, protecting it from denaturation (occurring under dry conditions) and nonspecific adsorption.[28] Different types of enzymatic composites have been synthesized using various methods. Glucose-oxidase (GOX)/PEG composites have been obtained by combining covalent surface immobilization and hydrogel entrapment or physical entrapment and covalent immobilization.[26,28] At the same time, it is possible to use as support for enzyme immobilization simultaneously with the hydrogel an inorganic support. Thus,

Table I. The Recipes Used for the Synthesis of the Hydrogel Samples

	Monomer concentration in water, (%)		Mass ratio crosslinker/monomer			Percentage ratio initiator system component/monomer, (%)		
Sample	AA	MA	MBA	EGDMA	GA	MS	KPS	$FeSO_4 \cdot 7H_2O$
HG 1		19.0	0.023			3.28	3.28	
HG 2		19.0		0.023		3.28	3.28	
HG 3		19.0	0.023			3.28	3.28	3.28
HG 4	19.5		0.021			3.17	3.17	
HG 5	19.5		0.042			3.17	3.17	3.17
HG 6	19.5		0.063			3.17	3.17	3.17
HG 7	19.5		0.084			3.17	3.17	3.17
HG 8	19.5				2.648	3.17	3.17	3.17
HG 9	19.5				4.238	3.17	3.17	3.17
HG 10	19.5			0.022		3.17	3.17	15.43

GOX-silica-PEG-based hydrogels composites have been synthesized.[28]

Enzymatic composites have also been obtained, using different enzymes (GOX, LOX, laccase, urease, carbonic anhydrase, or serum bovine albumin).[8,13,15–17,29–32] The hydrogels and the composites thus obtained have been characterized by scanning electron microscopy (SEM) and TGA.[9,10,18–20,24,26,28,32–34]

The aim of this study is to synthesize hydrogels in different conditions, using AA and methacrylic acid (MA) as monomers and to check the ability to obtain enzymatic composites by using these new products. Thus, a redox initiating system [sodium metabisulfite (MS)-potassium peroxydisulfate (KPS)] and different crosslinking agents [*N*,*N*′-methylene bisacrylamide (MBA), ethylene glycol dimethacrylate (EGDMA), and glutardialdehyde (GA)] have been used for hydrogels synthesis. Enzymatic composites have been synthesized using two enzymes: Horseradish peroxidase (HRP) and xylanase (XYL). The differences between hydrogels synthesized in different conditions, as well as between hydrogels themselves and hydrogels with immobilized enzymes were investigated by SEM, TGA, Fourier transform infrared (FTIR) spectrometry, DSC, and Raman spectrometry. The enzyme effect on the hydrogel composition and thermal behavior has been investigated, too.

EXPERIMENTAL

Materials

The monomers, AA and MA, were supplied by Merck (Darmstadt, Germany) and distilled for inhibitor removing. The components of the redox initiation system: KPS, MS and optionally iron (II) sulfate ($FeSO_4 \cdot 7H_2O$), pro-analysis, were received from "Reactivul" (Bucharest, Romania) and used as received. The crosslinkers MBA, EGDMA more than 99% purity, were purchased from Merck (Darmstadt, Germany) and used without further purification. GA, aqueous solution 50% was purchased from Merck (Darmstadt, Germany) and used as received.

The enzymes XYL, provided by Sigma-Aldrich (St. Louis) and HRP, provided by Merck (Darmstadt, Germany), were used as received.

Sample Synthesis

It was extensively studied the possibility of synthesizing samples of hydrogels using two monomers (AA or MA) and two variants of initiating systems or different crosslinking agents. Different from the literature,[35] we used a redox initiating system for hydrogel synthesis, not ammonium peroxydisulfate. We have changed the initiator system because of the drawbacks of the previous system, that would have involved making the polymerization at 50°C. Using a redox initiating system, the polymerization takes place at room temperature. At the same time, the polymerization rate increases. We have also used three crosslinkers and we have extended the method to MA. To synthesize acrylic hydrogels, the specified water amount was introduced in the reaction vessel. Then the monomer (AA or MA) was added, followed by the addition of the crosslinking agent and finally the initiating system was added, as aqueous solutions (KPS solution was the last added). The reaction was carried out in air, as preliminary tests of polymerization in a nitrogen atmosphere revealed no influence of oxygen. Polymerization took place at room temperature (22°C) during 10 min.

The recipes used for hydrogels synthesis are given in Table I.

Enzyme Immobilization

To covalently immobilize XYL or HRP, an enzyme solution was first prepared by dissolving 5 mg enzyme in 6 mL phosphate buffer solutions. Phosphate buffer 0.1*M* pH = 7 (synthesized using $NaH_2PO_4 \cdot 2H_2O$ 0.1*M* and KH_2PO_4 0.1*M*) was used for HRP dissolution. Phosphate buffer 0.1*M* pH = 9 (synthesized using $Na_2B_4O_7 \cdot 10H_2O$ 0.1*M* and KH_2PO_4 0.1*M*) was used for XYL dissolution, because only at such high pH XYL forms a colloidal solution, necessary for the covalent immobilization. According to the literature,[36–38] XYL exhibits a good resistance to alkaline pH. For some XYL sorts, the optimal activity occurs at pH = 9. The immobilization stage consisted of putting the enzyme solution in contact with 50 mg hydrogel sample for 2 h at room temperature. After that, the samples were intensively washed with water and buffer to remove the absorbed or adsorbed enzyme. Tests using acrylic hydrogel- XYL composites for the depolymerization of beach wood xylan were performed

Table II. Main FTIR Bands for Pure Enzymes, Pure Hydrogels, and Hydrogels With Immobilized Enzymes

Sample	υ_{OH} (from hydroxyl)	$\upsilon_{C=O}$ (from carbonyl)	$\upsilon_{C=O}$ (from amide I)	$\upsilon_{C=O}$ (from amideII)
XYL	3351	-	1643	1542
HRP	3288	-	1653	1536
HG 1	3400	1698	1640	1551
HG1-HRP	3391	1698	1655	1532
HG1-XYL	3385	1698	1646	1551
HG 2	3369	-	1649	-
HG 2-XYL	3364	-	1644	1545
HG 3	3383	1705	1652	-
HG 4	3114	1705	-	-
HG 5	3385	1702	1631	-
HG 5-XYL	3366	-	1637	-
HG 6	3383	1710	1635	-
HG 6-XYL	3416	1705	1653	1550
HG 7	3387	1696	1635	-
HG 7-XYL	3364	1701	-	1545
HG 8	3458	1696	-	-
HG 9	3453	1719	-	-

at pH = 9 (because at pH < 9, beach wood xylan is insoluble), proving the activity of the enzyme in multiple incubations (data not shown).

Sample Characterization

Fourier Transform Infrared Spectrometry. The Fourier Transform Infrared (FTIR) spectra were registered on a BRUKER VERTEX 70 (Ettlingen, Germany) equipment using 32 scans with 4 cm^{-1} resolution in 400–4000 cm^{-1} region. The samples were analyzed using ATR unit.

Raman Spectroscopy. The Raman spectra were recorded on a DXR model Raman microscope, equipped with Omnic 8 software from Thermo Fisher Scientific (Madison, WI), with a signal to noise ratio of 100. The excitation laser wavelength was 780 nm, using a laser power level of about 10 mW. The Raman spectra were recorded in 50–3550 cm^{-1} region.

Scanning Electron Microscopy. SEM images were obtained on VEGA II XMU Tescan (Brno, Czech Republic) microscope at an accelerating voltage of 30 kV. The SEM microscope was used to investigate the hydrogels themselves and hydrogels with immobilized enzymes morphology.

Differential Scanning Calorimetry. The differential scanning calorimetry (DSC) curves were registered on a Netzsch DSC 204 F1 Phoenix (Selb, Germany) using a heating rate of 10°C/min. Each sample was heated from 20 to 180°C, under a constant nitrogen flow rate (40 mL/min.).

Thermo Gravimetric Analysis and Differential Thermal Gravimetry. The thermo gravimetric analysis (TGA) and differential thermal gravimetry (DTG) results were obtained simultaneously on a Q 500 TA instrument (New Castle, DE). A typical sample was heated from 20 to 400°C at heating rate of 10°C/min under a constant nitrogen flow rate (100 mL/min).

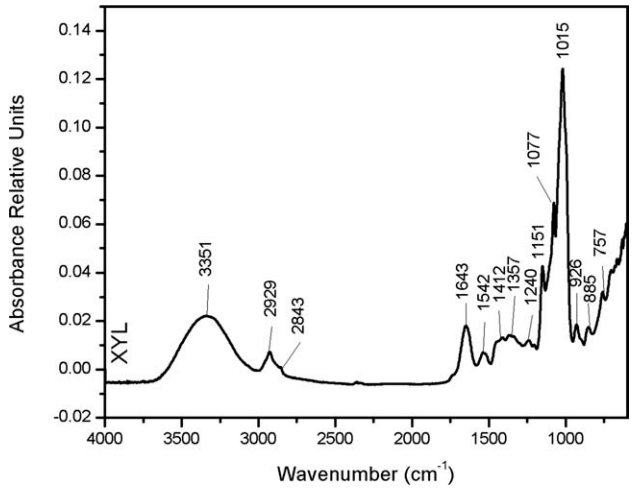

Figure 1. FTIR spectra of pure XYL.

RESULTS AND DISCUSSION

Chemical Composition Investigation

To determine the composition of the synthesized hydrogels and to prove the XYL and HRP immobilization on these hydrogels, FTIR spectra were recorded for different hydrogels before and after the enzyme immobilization and for enzymes themselves. FTIR data for all samples are given in Table II. Figures 1 and 2 present the FTIR spectra of pure enzymes (XYL and HRP, respectively).

Comparing the FTIR spectra of pure and enzyme modified hydrogels from Figure 3, one may notice that:

- All three samples exhibit peaks at ~ 3400 cm^{-1}, which are assigned to —OH groups from polymethacrylic acid (PMA).
- For the pure hydrogel, peaks assigned to $—CH_2—$ stretching vibration appear at 2923 cm^{-1} and 2846 cm^{-1}. After the immobilization of XYL or HRP, the vibration intensity seems to be reduced.

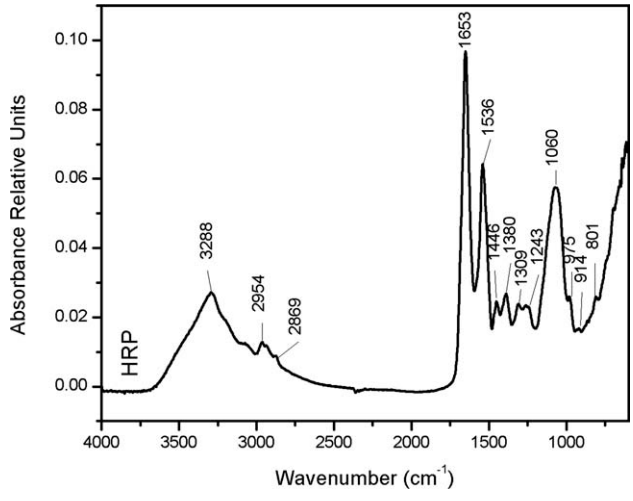

Figure 2. FTIR spectra of pure HRP.

Applied Polymer SCIENCE

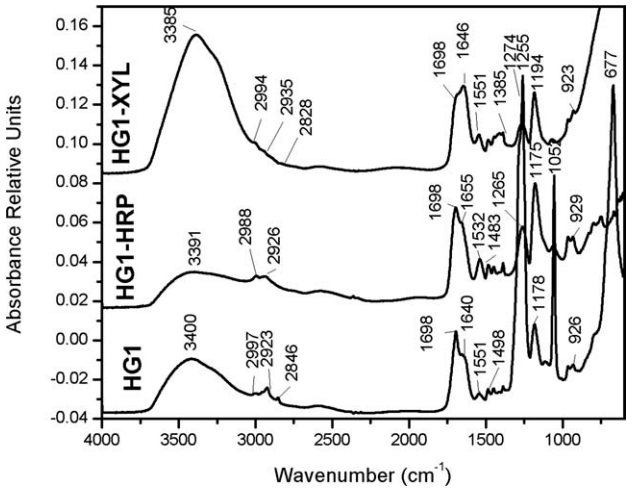

Figure 3. FTIR spectra for pure HG 1, for HG 1 with immobilized xylanase (HG1-XYL) and for HG1 with immobilized horseradish peroxidase (HG1-HRP).

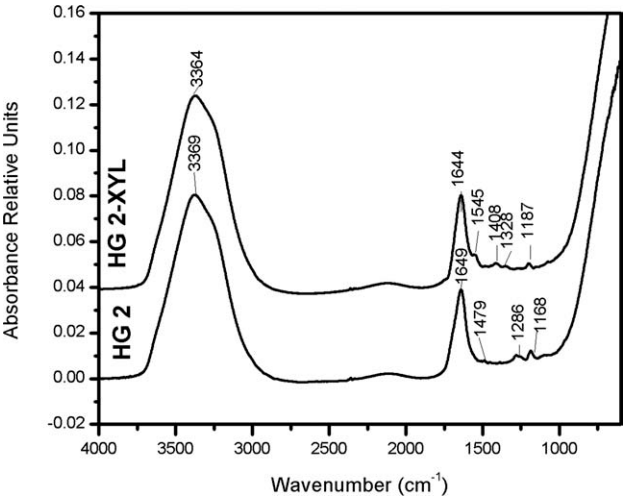

Figure 4. FTIR spectra of HG 2 and HG2 with immobilized xylanase (HG2-XYL).

- For pure hydrogel, it appears a peak at 1698 cm^{-1} which is assigned to C=O groups from PMA. This peak also occurs in the FTIR spectra of HG1-HRP sample and also in HG1-XYL spectra.
- Peaks assigned to peptide groups appear for all samples at about 1650 and at 1550 cm^{-1}. In case of pure XYL (Figure 1) a peak appears between 1500 and 1550 cm^{-1} (at 1542 cm^{-1}) because the enzyme is formed of amino acid chains. For hydrogel, the peptide groups are formed after crosslinking with MBA and, for the samples of hydrogel with immobilized enzyme a superposition of the peptide group formed in these two ways takes place.
- For HG1-HRP, a peak appears at 929 cm^{-1}, which in HRP spectra appears at 914 cm^{-1}. This peak is assigned to C—O bonds from the amino acids existing in HRP. At the same time, HG1-XYL, also, exhibits a peak (at 923 cm^{-1}) assigned to C—O bonds from the amino acids from XYL (at 926 cm^{-1}). Because HG1 exhibits, also, a peak at 926 cm^{-1}, FTIR method cannot confirm the enzyme immobilization for HG1 composites.
- From Figure 4, one may notice that:
- Both samples, HG2 and HG2-XYL exhibit peaks at 3360–3370 cm^{-1} (which are assigned to —OH groups from PMA) and at 1644–1649 cm^{-1} (assigned to —C=O groups from PMA superposed on —C=O from the crosslinker EGDMA; for HG2-XYL sample this peak may be also assigned to —C=O from the amino acids contained by the enzyme).
- After XYL immobilization, a new peak appears at 1545 cm^{-1}. This peak is assigned to peptide groups and it occurs in the enzyme FTIR spectra at 1542 cm^{-1}. The presence of a peak which is characteristic to the enzyme proves that the immobilization took place.

Comparing the FTIR spectra of two hydrogels based on different monomers (MA and AA), the following features are observed (Figure 5):

- For HG 3, a peak appears at 3383 cm^{-1} which is assigned to —OH groups from MA. This peak is less developed in the spectra of HG 4, and shifted to a lower value, proving that the crosslinking reaction with MBA can alter —OH groups from PAA.
- For HG 4 a peak appears at 1705 cm^{-1} which is assigned to carbonyl groups from AA. This peak is replaced in HG 3 spectrum by a two peaks band at 1705 and 1652 cm^{-1}. The carbonyl groups from MA are consumed by reaction with —NH_2 groups from MBA during crosslinking leading to peptide groups formation (a new peak appears at 1652 cm^{-1}). So, one may presume that the crosslinking takes place in a different way for the two polyacids.

Comparing the FTIR spectrum of HG 5 (Figure 6) to the spectrum of HG5-XYL, one may notice that after enzyme immobilization carboxyl groups are transformed into amide groups because the two peaks from 1702 and 1631 cm^{-1} are replaced by a single peak at 1637 cm^{-1}. This confirms that the immobilization took place.

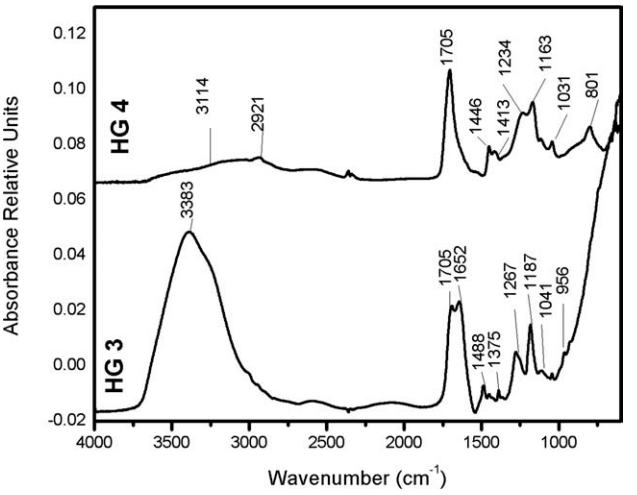

Figure 5. FTIR spectra of HG 3 (hydrogel based on MA) and HG 4 (hydrogel based on AA).

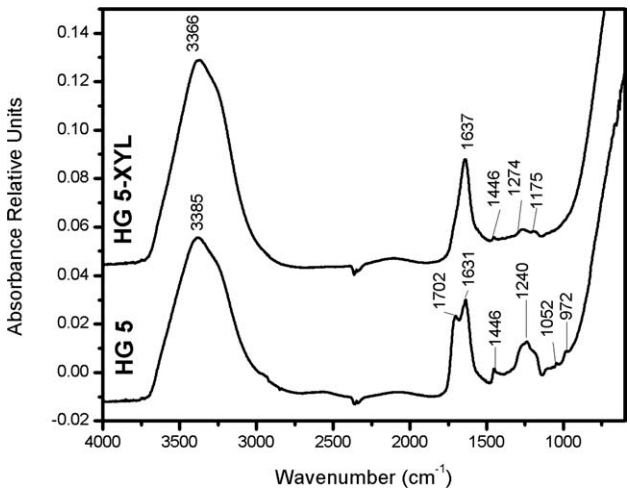

Figure 6. FTIR spectra for HG 5 itself and HG 5 with immobilized xylanase (HG 5-XYL).

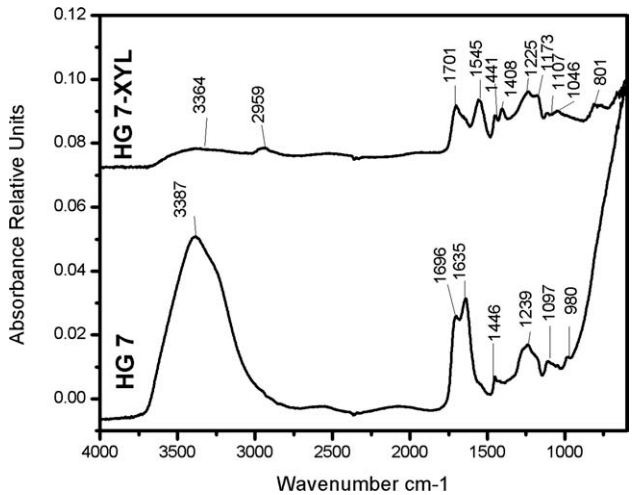

Figure 8. FTIR spectra for HG 7 itself and HG 7 with immobilized xylanase (HG 7-XYL).

Comparing the FTIR spectrum of HG 6 to the spectrum of HG6-XYL (Figure 7), one may notice that:

- After XYL immobilization the peak from ~ 3400 cm^{-1} assigned to —OH groups diminishes proving changes in the chemical composition and suggesting a participation of OH groups in the immobilization.
- After XYL immobilization, the peaks assigned to C=O groups appearing at 1710 shifts to 1705 cm^{-1} and the peptide groups peaks change from 1635 to 1653 cm^{-1}, respectively. It is noteworthy that the immobilization changes the ratio between C=O band and peptide band.
- The XYL immobilization is also confirmed by the presence of a peak at 1550 cm^{-1} (assigned to peptide groups) in the spectrum of HG6-XYL, which is missing in HG6 spectrum.

Comparing the FTIR spectrum of HG 7 to the spectrum of HG7-XYL (Figure 8), one may notice that:

- After XYL immobilization the peak of —OH groups from 3360–3390 cm^{-1} decreases dramatically, showing again changes in the chemical composition and suggesting again a participation of OH groups in the immobilization.
- A new peak appears at 1545 cm^{-1} in the spectrum of HG7-XYL. This peak is characteristic to the enzyme, being assigned to peptide groups, and its presence confirms the enzyme immobilization.
- The peak from 1635 cm^{-1} (which is assigned to peptide I groups) disappears after the enzyme immobilization. A possible explanation is that, like in the previous case (Figure 7) a change of the ratio between the two bands at 1696 and 1635 takes place and in the enzyme composite the amide I peak is included in a larger —C=O peak.

The FTIR spectra of the two hydrogels synthesized using different amounts of GA crosslinker (Figure 9), show that these two samples exhibit the same peaks, so the amount of crosslinking agent does not influence the chemical composition.

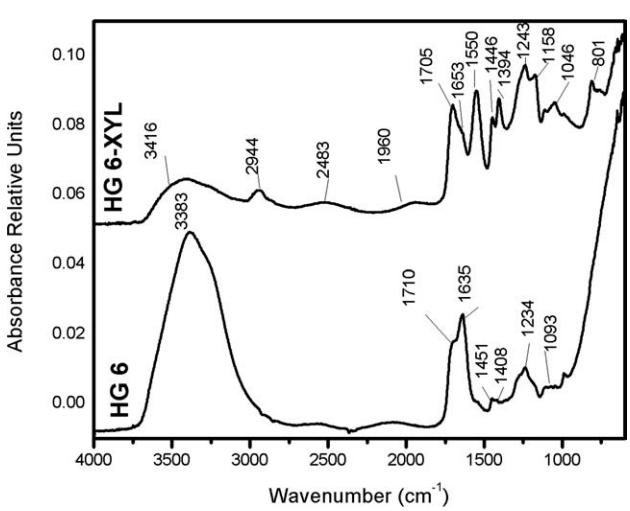

Figure 7. FTIR spectra for HG 6 itself and HG 6 with immobilized xylanase (HG 6-XYL).

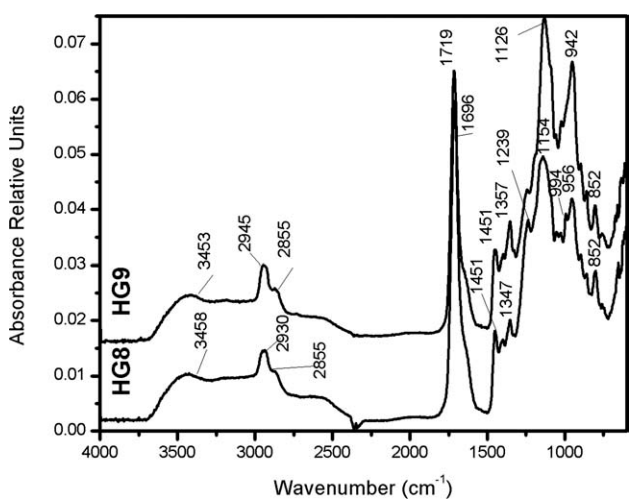

Figure 9. FTIR spectra for hydrogels synthesized using different crosslinking agent (GA)/monomer (AA) mass ratios: HG 8(GA/AA = 2.648), HG 9(GA/AA = 4.238).

Applied Polymer SCIENCE

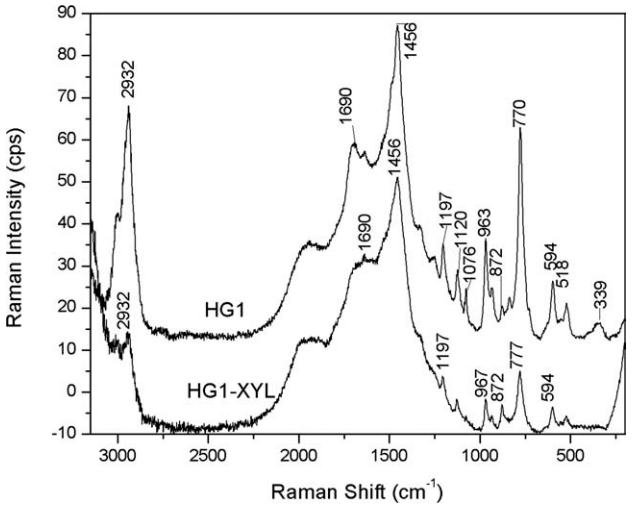

Figure 10. Raman spectra of HG 1 itself and of HG 1 with immobilized xylanase (HG1-XYL).

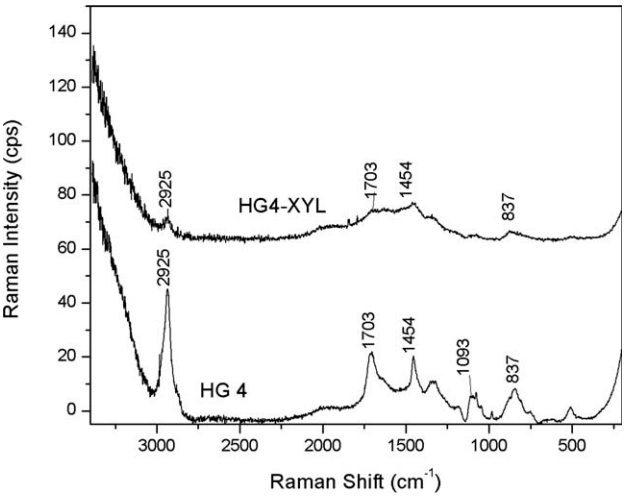

Figure 12. Raman spectra of HG 4 itself and of HG 4 with immobilized xylanase (HG4-XYL).

Comparing the results in Table II and Figures 3–9, it is noteworthy that the two polyacids exhibit a slight difference in the enzyme immobilization behavior. PAA is a stronger acid than PMA, because the presence of —CH_3 groups leads to an acid character decrease. For PAA (the stronger acid) the —OH groups participation for enzyme immobilization is more obvious.

To further investigate the chemical composition of the hydrogels, before and after enzyme immobilization, the Raman spectra were recorded. Comparing the Raman spectra of HG 1 itself to the spectra of HG 1-XYL (Figure 10), the following features are observed:

- The peak from 2932 cm^{-1} is present in both spectra. This peak is assigned to methylene groups from PAA and it is less intense in the case of hydrogel with enzyme.
- The peak from 1690 cm^{-1}, assigned to carbonyl groups, is also present in both spectra, but its intensity is reduced after enzyme immobilization, these groups being transformed during the immobilization reaction.
- At 1456 cm^{-1} a peak appears in both spectra. This peak is assigned to vinyl bonds from the monomer and the MBA crosslinking agent.
- The peak at 1197 cm^{-1} is present in both spectra and is assigned to C—C bond vibration. This peak is diminished in the spectrum of HG 1-XYL, perhaps because after enzyme immobilization, the backbone vibration is reduced.
- Peaks assigned to SO_4^{2-} ions from the initiating redox system appear at 967, 872, 777 (for HG1-XYL) and at 963, 872, 770 cm^{-1} (for HG1).
- Peaks assigned to OH groups appear at 594 and 518 cm^{-1} in both spectra, but their intensity is reduced after enzyme immobilization, being used in the immobilization reaction.

The immobilization of the enzyme is confirmed by the fact that the intensity of the peaks assigned to carbonyl and hydroxyl groups decreases after immobilization.

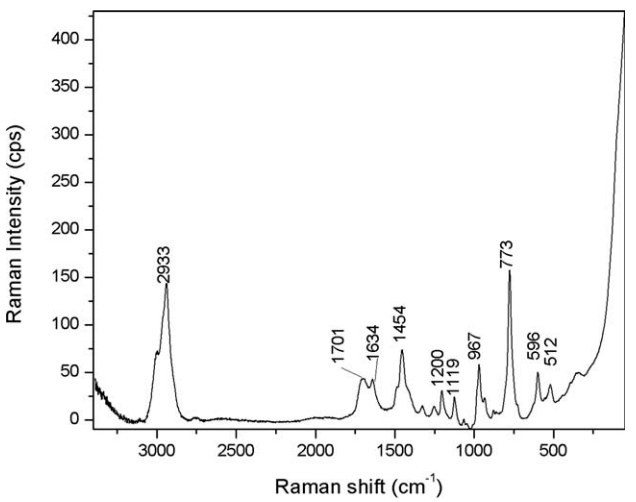

Figure 11. Raman spectra of HG 3.

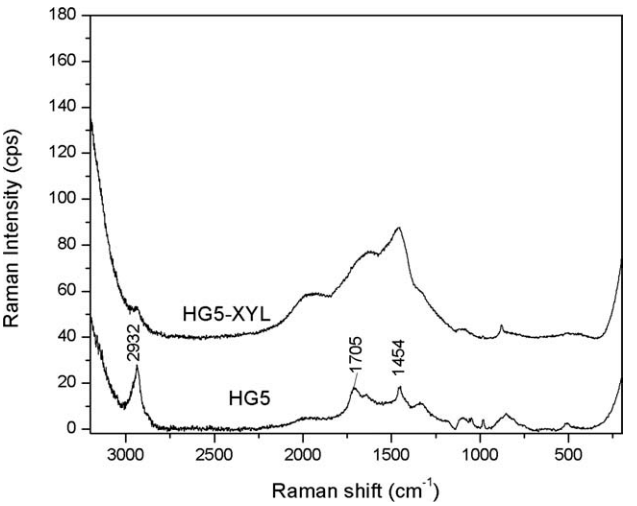

Figure 13. Raman spectra of HG 5 itself and of HG 5 with immobilized xylanase (HG5-XYL).

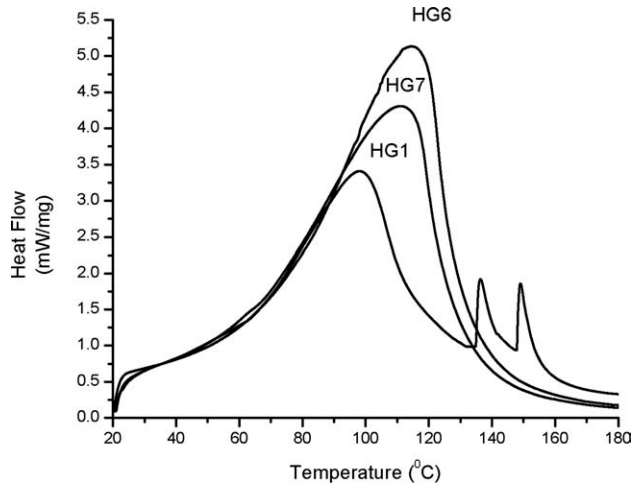

Figure 14. DSC curves of three hydrogels synthesized using different monomers and different MBA/monomer mass ratios: HG1 (MBA/MA = 0.023); HG6 (MBA/AA = 0.063); HG7 (MBA/AA = 0.084).

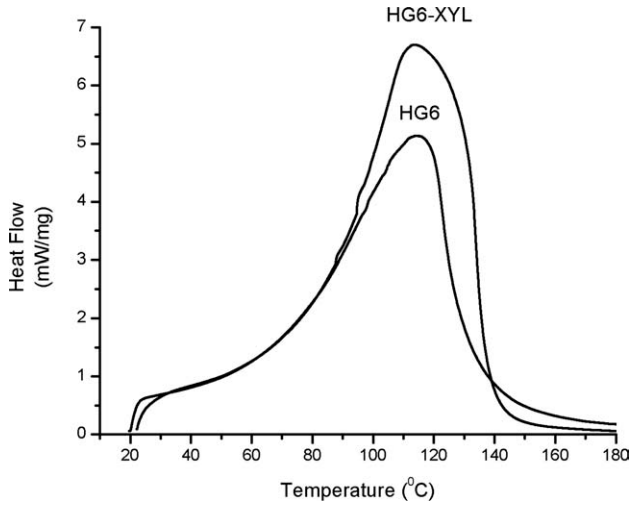

Figure 15. DSC curves for HG 6 itself and HG6 with immobilized xylanase (HG6-XYL).

As it can be noticed from Figure 11, HG 3 exhibits peaks at:

- 2933 cm^{-1}, assigned to methylene groups from the monomer and the crosslinking agent;
- 1701 cm^{-1}, assigned to C—O bonds from the hydrogel;
- 1634 cm^{-1}, assigned to amide I bond;
- 1454 cm^{-1}, assigned to vinyl bonds from the monomer and the crosslinking agent;
- 1200, 1119, 967, and 773 cm^{-1}, assigned to SO_4^{2-} groups from the initiator system;
- 596 and 512 cm^{-1}, assigned to OH groups.

Comparing the Raman spectrum of HG4 to the spectrum of HG4-XYL (Figure 12), one may notice that:

- A peak appears at 2925 cm^{-1} in both spectra. This peak is assigned to methylene groups and diminishes dramatically after the immobilization.
- A peak appears at 1703 cm^{-1} in both spectra, but after enzyme immobilization its intensity decreases. This peak is assigned to C═O groups from the hydrogel, which are transformed during enzyme immobilization. Thus, the enzyme immobilization is confirmed.
- A peak assigned to vinyl bonds from the monomer and the crosslinking agent appears in both spectra at 1454 cm^{-1};
- Peaks assigned to SO_4^{2-} (from the initiator system) appear in both spectra at 1093 and 837 cm^{-1}.

Comparing the Raman spectra of HG 5 before and after the immobilization of XYL (Figure 13), the following features are observed:

- A peak assigned to methylene groups appears in both spectra at 2932 cm^{-1}, but its intensity decreases after enzyme immobilization.
- Peaks assigned to carbonyl groups appear in both spectra at 1705 cm^{-1}. The intensity of the peak decreases after the enzyme immobilization, carbonyl groups being transformed during immobilization by the reaction of —COOH with —NH_2 groups from the enzyme.
- Peaks assigned to vinyl bonds (from the monomer and the crosslinking agent) appear in both spectra at 1454 cm^{-1}.

Thermal Behavior Investigation

To check the synthesis conditions and the enzyme influence on the thermal behavior of the hydrogels, the DSC curves were recorded for three samples of hydrogels synthesized in different conditions (Figure 14) and for one of these hydrogels before and after the enzyme (XYL) immobilization (Figure 15). The temperatures and the areas assigned to the peaks from the DSC curves are given in Table III. As it can be noticed from Figure 14 and Table III, only HG 1 (MA based) exhibits three peaks (at 98, 136, and 149°C). The first peak may be assigned to water evaporation (T_v). The second and the third peak may be assigned to the melting points (T_m). So, melting takes place in two stages, at around 136°C and 149°C, respectively, this may be due to the heterogeneity of the crosslinking.

For the two samples of AA based on hydrogel, only one peak appears and it is assigned to the water evaporation. HG6 is synthesized using a lower amount of crosslinking agent than HG 7.

Table III. The Temperatures and the Areas Assigned to the Peaks From the DSC Curves

	Peak 1		Peak 2		Peak 3	
Sample	Temperature (°C)	Area (J/g)	Temperature (°C)	Area (J/g)	Temperature (°C)	Area (J/g)
HG 1	98	588.3	136.4	25.81	149	20.91
HG 6	114.5	1259	–	–	–	–
HG 7	111.2	1143	–	–	–	–
HG 6-XYL	113.6	1741	–	–	–	–

Applied Polymer SCIENCE

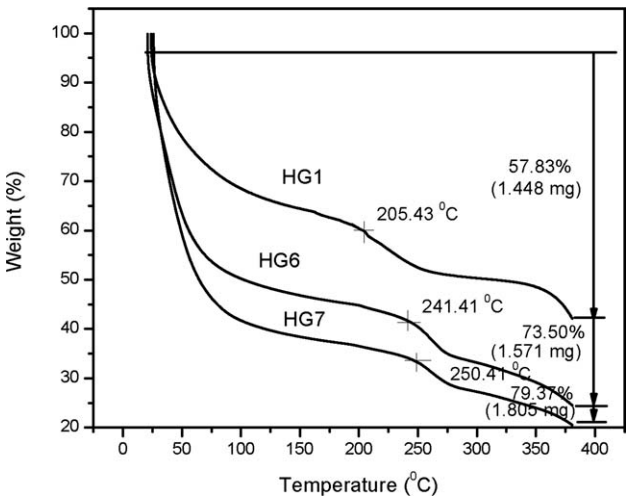

Figure 16. TGA curves of three hydrogels synthesized using different monomers and different MBA/monomer mass ratios: HG1 (MBA/MA = 0.023); HG6 (MBA/AA = 0.063); HG7 (MBA/AA = 0.084).

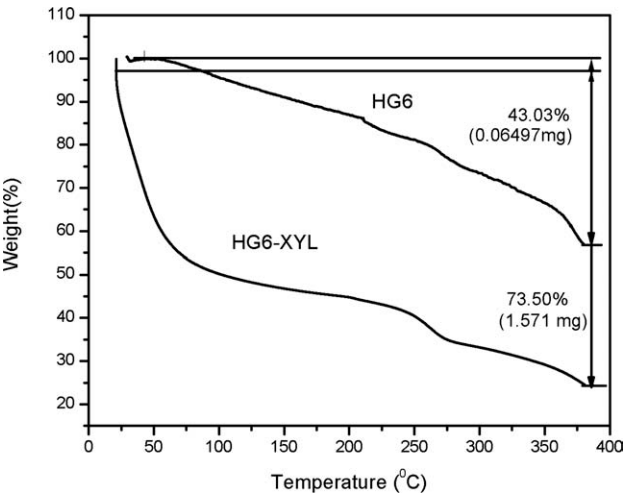

Figure 18. TGA curves of HG 6 itself and HG 6 with immobilized xylanase (HG6-XYL).

The maximum of the evaporation temperature (T_v) for these samples are rather close so that one can say that the thermal behavior of the hydrogels is much more influenced by the nature of formed polyacid than by the crosslinker amount. Anyway, with the increase of crosslinking agent content, it can be noticed a slight decrease in the T_v value. The hydrogel water retention capacity could be estimated from the water vaporization peak area (see Table III). HG1 (MA based) exhibits a smaller water retention (thermal effect 588 J/g) than HG6 and HG 7 (AA based). In the case of AA-based hydrogels, as expected the water content is reduced (thermal effect decreases from 1259 J/g for HG6 to 1143 J/g for HG7).

As it can be noticed from Figure 15, after the enzyme immobilization the evaporation temperature decreases only from 114.5 to 113.6°C, showing that the enzyme does not influence the evaporation point. But, the thermal effect increases from 1259 to 1741 J/g, showing that the enzyme immobilization leads to an enhancement of the hydrophilic character.

To further confirm the differences in the thermal behavior of the three samples of hydrogel synthesized in different conditions, the TGA and DTG curves (Figures 16 and 17) were recorded for the same three hydrogels: HG1, HG6, and HG7. No important modifications are noticed in TGA curves (Figure 16) for HG6 and HG7 samples, what proves once again that the amount of the crosslinking agent does not lead to important changes in the thermal behavior. The differences in the thermal behavior of the MA-based hydrogel (HG1) and the two samples of AA based on hydrogels (HG6 and HG7) are due to the different chemical composition, but perhaps, also, to the different crosslinking agent amounts, because HG 1 exhibits the lowest crosslinking agent amount. As it can be noticed from Figure 17, HG 1 (MA based on hydrogel) exhibits three main peaks at about 165, 207, and 223°C. The two other samples, HG 6 and HG 7 (AA based on hydrogels) exhibit only two peaks: one

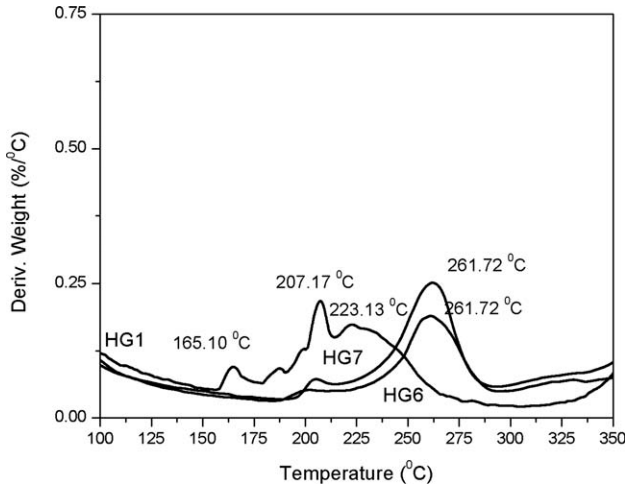

Figure 17. DTG curves of three hydrogels synthesized using different monomers and different MBA/monomer mass ratios: HG1 (MBA/MA = 0.023); HG6 (MBA/AA = 0.063); HG7 (MBA/AA = 0.084).

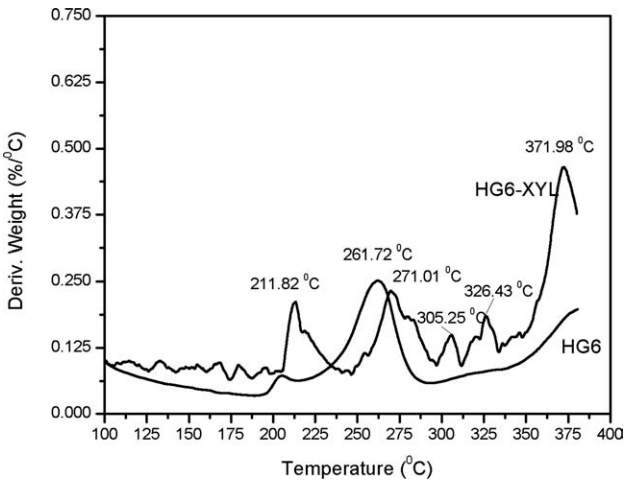

Figure 19. DTG curves of HG 6 itself and HG 6 with immobilized xylanase (HG6-XYL).

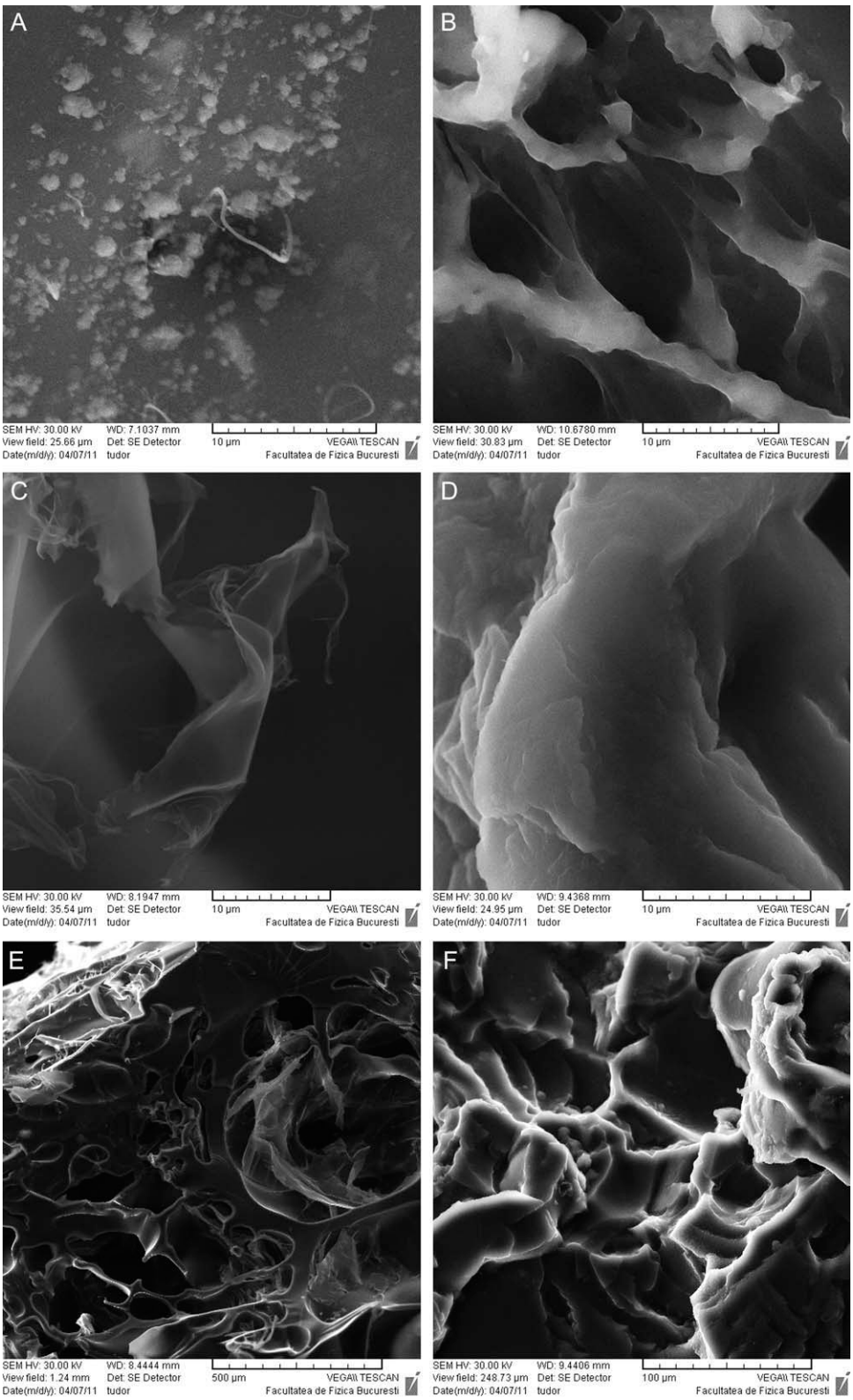

Figure 20. SEM images of pure hydrogels and hydrogels with immobilized enzymes recorded at different magnifications (A–D at 10 μm; E-500 μm; F-100 μm). (A) HG 1; (B) HG 4; (C) HG1-HRP; (D) HG6-XYL; (E) HG1-HRP; (F) HG6-XYL.

small peak at about 200°C and another peak at about 262°C. The MA based on hydrogel is more stable than the AA based on hydrogels, even though it exhibits more decomposition stages but the final loss of weight is lower (Figures 16 and 17).

To further check how the enzyme influences the thermal behavior of hydrogels, the TGA and DTG curves (Figures 18 and 19) were recorded for HG 6 before and after the covalent immobilization of XYL.

As it can be noticed from Figures 18, and 19, the thermal degradation takes place faster for HG 6-XYL than for HG 6 and it occurs during several stages. This is due to the fact that the enzyme (XYL) is a proteine and it exhibits a low thermal resistance.

Morphology Investigation

To compare the morphology of hydrogels synthesized in different conditions and to see how the immobilization of an enzyme affects the morphology of the hydrogel, SEM images were recorded (Figure 20). To further investigate the morphology of the samples with immobilized enzyme the SEM images for these samples were also recorded at lower magnifications.

Comparing the SEM images recorded for a magnification of 10 μm, the following features are observed:

- HG 1 itself exhibits a non-homogenous morphology. After the immobilization of HRP, important changes are noticed. The white areas may be assigned to the enzyme presence.
- HG 4 exhibits a sponge like morphology. Thus, the structure confirms the enhanced water retention of AA based on hydrogels (observed in DSC, Table III), because this porous structure allows water retention.
- HG6-XYL exhibits white areas, which similarly to HG1-HRP, may be assigned to the enzyme presence. Thus, the immobilization is confirmed.

Both samples with immobilized enzyme exhibit a similar morphology. For both samples (HG1-HRP and HG6-XYL) when the resolution is decreased (500 and 100 μm, respectively) a sponge like morphology can be noticed. This morphology is due to the enzyme tridimensional structure.

CONCLUSIONS

AA- and MA-based hydrogels, crosslinked using different agents, can be used for enzyme immobilization without any activating agent.

The results obtained by Raman spectroscopy are in good agreement with those obtained by FTIR spectrometry, both methods confirming that the enzyme covalent immobilization can be performed on hydrogels.

The TGA results are in good agreement with the DSC results, proving that MA-based hydrogel is more stable than the two hydrogels based on AA. AA based hydrogels are more hydrophilic than MA based ones. The TGA and DSC curves also show the important influence of the used acid and that the amount of crosslinking agent does not lead to important changes in the thermal behavior of the hydrogel. The enzyme accelerates the thermal degradation of the biocomposite.

The SEM images show that the gel structure is porous and prove the immobilization of the enzyme.

ACKNOWLEDGMENTS

The work has been funded by the Sectoral Operational Programme Human Resources Development 2007-2013 of the Romanian Ministry of Labour, Family and Social Protection through the Financial Agreement POSDRU/88/1.5/S/61178. This work was also supported by the BS Eranet project 7-045 IMAWATCO and by the UEFISCDI, ROMANIA (P. D. Grant No. 15/2010).

REFERENCES

1. Sadeghi, M.; Heidari, B. *Materials* **2011,** *4*, 543.
2. Kim, I. Y.; Kim, S. J.; Shin, M. S.; Lee, I. M.; Shin, D. I.; Kim, S. I. *J. Appl. Polym. Sci.* **2002,** *85*, 2661.
3. Ozkahraman, B.; Acar, I.; Emik, S. *Polym. Bull.* **2011,** *66*, 551.
4. Zhang, J.; Peppas, N. A. *J. Appl. Polym. Sci.* **2001,** *82*, 1077.
5. Kwon, D.Y.; Kim, W. Y. *J. Biochem. Mol. Biol.* **1996,** *29*, 163.
6. Francis, S., Kumar, M.; Varshney, L. *Radiat Phys. Chem.* **2004,** *69*, 481.
7. He, G.; Zheng, H.; Xiong, F. *J. Wuhan Univ. Technol.* **2008, 816.**
8. Abbasi, F.; Jalili, K.; Alinejad, Z.; Alizadeh, M. *Iran J. Chem. Eng.,* **2010,** *7*, 3.
9. Krishna Rao, K. S. V.; Ha, C. S. *Polym. Bull.,* **2009,** *62*, 167.
10. Nieto, M.; Nardecchia, S.; Peinado, C.; Catalina, F.; Abrusei, C.; Gutiérrez, M. C.; Ferrer, M. L.; del Monte, F. *Soft. Mater.,* **2010,** 3533.
11. Kim, S. J.; Lee, K. J.; Kim, I. Y.; An, K. H.; Kim, S. I. *J. Appl. Polym. Sci.* **2003,** *90*, 1384.
12. Kim, I. S.; Oh, I. J. *Arch. Pharm. Res.* **2005,** *28*, 983.
13. De Giglio, E.; Cometa, S.; Cioffi, N.; Torsi, L. *Anal. Bioanal. Chem.* **2007,** *389*, 2055.
14. Saraç, A. S.; Ustamehmetođlu, B.; Sezer, E.; Erbil, C. *Tr. J. Chem.* **1996,** *20*, 80.
15. Lu, Y.; Wang, D.; Tao, L.; Xuqing, Z.; Yuliang, C.; Hanxi, Y.; Duan, Y. Y. *Biomaterials* **2009,** *30*, 4143.
16. Coffey, A.; Stanley, C.; Walsh, P. Society of Plastics Engineering, Plastics Research Online. Available at: http://www.4spepro.org/pdf/003334/003334.pdf, accessed February 12, **2012.**
17. Sadeghi, M.; Soleimani, F. *Int. J. Chem. Eng. Appl.* **2011,** *2*, 304.
18. Gürel, I.; Arica, M. Y.; Hasirci, V. *Tr. J. Chem.* **1997,** *21*, 387.
19. Gai, L.; Daocheng, W. *Appl. Biochem. Biotechnol.* **2009,** *158*, 747.
20. Yan, J.; Pedrosa, V. A.; Simonian, A. L.; Revzin, A. *Appl. Mater. Interface* **2010,** *23*, 748.
21. Can, H. K.; Denizli, B. K.; Güner, A.; Rzaev, Z. M. O. *Hacettepe J. Biol. Chem.* **2009,** *37*, 145.

22. Omidian, H.; Park, K.; Kandalam, U.; Rocca, J. G. *J. Bioact. Compat. Polym.* **2010,** *25*, 483.
23. Pooley, S. A.; Rivas, B. L.; Lillo, F. E.; Pizzaro, G. D. C. *J. Chil. Chem. Soc.* **2010,** *55*, 19.
24. Zhang, Y. T.; Fan, L. H.; Zhi, T. T.; Zhang, L.; Huang, H.; Chen, H. L. *J. Polym. Sci.* **2009,** *47*, 3232.
25. Jovanović-Malinovsko, R.; Amartey, S. A.; Kuzmanova, S.; Winkelhausen, E.; Cvetovska, M.; Tsvetanov, C. *Bull. Chem. Technol. Macedonia* **2006,** *25*, 113.
26. Choi, D.; Lee, W.; Lee, Y.; Kim, D. N.; Park, J.; Koh, W. G. *J. Chem. Technol. Biotechnol.* **2008,** *83*, 252.
27. Sheldon, R. A. *Adv. Synth. Catal.* **2007,** *349*, 1289.
28. Jang, E.; Park, S.; Lee, Y.; Kim, D. N.; Kim, B.; Koh, W. G. *Polym. Adv. Technol.* **2010,** *21*, 476.
29. Smirnov, M. A.; Bobrova, N. V.; Dmitriev, I. Y.; Bukolšek, V.; Elyashevich, G. K. *Polym. Sci. Ser. A* **2011,** *53*, 67.
30. Baranovskii, V. Y.; Yasina, L. L.; Motyakin, M. V.; Aliev, I. I.; Shenkov, S.; Dimitrov, M.; Lambov, N.; Wasserman, A. M. *Polym. Sci. Ser. A* **2006,** *48*, 1304.
31. Jafari, S.; Madarress, H. *Iran Polym. J.* **2005,** *14*, 863.
32. Pourjavadi, A.; Soleyman, R.; Barajee, G. R. *Starch/Stärke* **2008,** *60*, 467.
33. He, H.; Li, L.; Lee, L. J. *Polymer* **2006,** *47*, 1612.
34. Diez-Pena, E.; Quijada-Garrido, I.; Barrales-Rienda, J. M. *Polym. Bull.* **2002,** *48*, 83.
35. Teodorescu, M.; Lungu, A.; Stanescu, P. O.; Neamtu, C. *J. Amer. Chem. Soc. Ind. Eng. Chem. Res.* **2009,** *48*, 6527.
36. Kaur, H.; Dutt, D.; Tyagi, C. H. *BioRes.* **2011,** *6*, 1376.
37. Gessesse, A.; Mamo, G. *J. Ind. Microbiol. Biot.* **1998,** *20*, 210.
38. Coral, G.; Arikan, B.; Ünaldi, M. N.; Korkmaz Güvenmez, H. *Ann. Microbiol.* **2002,** *52*, 299.